REVERSE BIAS DAMAGE IN CIGS MODULES

P-O. Westin, U. Zimmermann, L. Stolt, M. Edoff
Ångström Solar Center, Div. Solid State Electronics
Uppsala University, P.O. Box 534, SE-75121 Uppsala, Sweden

ABSTRACT: When solar modules are partially shaded they will be under conditions of partial reverse bias. To test and evaluate the effect of reverse bias, CIGS thin film PV modules were placed under extreme conditions of reverse stress. Stressing caused modules to exhibit visible "wormlike" damages. These damages were caused by hot spot activity during reverse stress. Local heating resulted in pore formation and forced the hot spot to move within the cell. This effect appeared to cause intermixing of the top ZnO layer with the CIGS absorber. Some phase segregation of an undetermined, Cu rich compound was also found near the back contact. Electrically, the observed damages caused local shunt conductance to increase resulting in irreversibly reduced module fill factors.
Keywords: $Cu(InGa)Se_2$, Modules, Stability

1 INTRODUCTION

In recent years photovoltaic thin film technologies such as CdTe and CIGS have passed from promising laboratory performance to commercial introduction, taking considerable market shares, e.g. in the U.S. [1]. The established Si wafer technology offers extensive warranties for long-term performance and stability. Through qualification and accelerated stress testing, thin-film technologies must address potential problems for their products in the field. One risk which modules in the field face is partial shading resulting in reverse bias and hot-spot formation. In order to ensure the resistance of the modules in such events, part of the qualifying tests, such as IEC 61646, is focused on placing the module in a worst case scenario for shading.

Shading of cells in a module, during testing or in the field, tends to place them under a reverse bias condition as the voltage of the remaining (illuminated) cells drops across the shaded one(s). Previous work has shown that reverse stress causes mild losses in the Voc and FF of a shadowed cell which recovered under light soaking [2]. An increased saturation current in CIGS modules was found after reverse bias stressing [3]. Reverse characteristics of CIGS cells under illumination depended on the wavelength used and on various treatments such as light soaking and annealing [2]. Reverse stressing of CIS minimodules recovered completely with time and it was concluded that bypass diodes would not be necessary for safe operation [4]. Field testing of CIGS modules has lead to the observation of wormlike damages in CIGS modules [5].

2 EXPERIMENTAL

In this investigation we subjected CIGS modules and cells to reverse bias in the dark and in light conditions. The formation of wormlike damages was observed using IR thermography and analyzed using SEM and EDX.

2.1 Reverse stress

Modules of the size $10x12cm^2$ and cells $1x0.5cm^2$ were used in this investigation. Reverse characteristics were determined by a current-voltage sweep in dark conditions. Modules and cells were then placed with reverse bias under 4 different conditions, see Table I. The bias light intensity was ~$500W/m^2$. Reverse stress was maintained for a period of 15 minutes. During reverse stress the current was held constant and the voltage drop was monitored. The devices biased in the dark were also monitored using IR thermography in search of hot spots.

2.2 Analysis

IV characteristics of the modules and cells were determined before and after the reverse stressing, using flash or halogen lamp solar simulators. The frequently appearing wormlike damages (see Figure 1a) were investigated using optical microscopy and SEM with EDX capabilities. Using a Focused Ion Beam (FIB), a cross section of the layers within the defect could be made and analysed. Module samples were also fractioned into sub-cells with and without *visible* damages. The performance of these sub-cells was then determined by IV measurement.

In order to find a correlation between the electrical data and the thermographical data, the change in voltage drop across the devices was plotted together with the intensity of IR radiation from the hot spots.

2.3 P1 – a weakest link?

One hypothesis was that the P1 scribe line was the weak link in providing suitable conditions for breakdown, either by the formation of "walls" or "collars" on the scribe edges or by high e-fields in the points formed by adjacent laser pulses. In order to further explore this idea, cells on top of P1 scribe lines were manufactured and tested.

Table I – Summary of experimental conditions and visual damage rating.

Group	Light/Dark	Rev. I	Rev. bias	Rating
A	Dark	-Jsc	2-3V/cell	Low
B	Dark	-½Jsc	2-3V/cell	High
C	Light	-Jsc	2-3V/cell	Medium
D	Light	-½Jsc	0.2-1.5V/cell	Medium

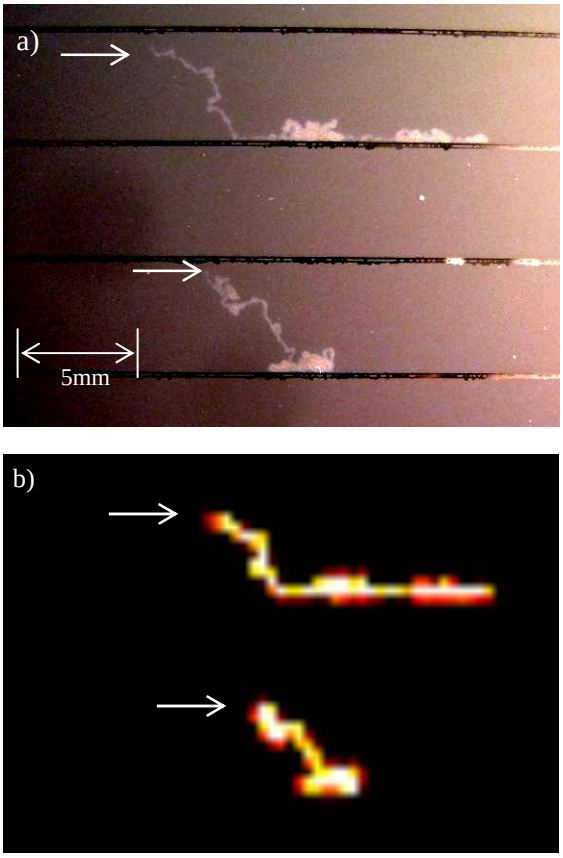

Figure 1 – Comparison of the visually observed damage (a) with a IR thermography trace (b) of moving hot spots during reverse stress. Arrows indicate the points of origin.

3 RESULTS and DISCUSSION

3.1 Visual inspection

In modules, visible wormlike damage was observed for all test conditions, groups **A-D**. Visual appreciation of the magnitude of the damage rated the dark, low-current samples (group **B**) as the most severely degraded, and the dark, high-current samples (group **A**) as the least degraded, quite contrary to expectations. Of course, a low level of visual damage does not necessarily imply low levels of performance degradation. Wormlike damages extended several mm:s in length and seemed to be present in each cell of a reverse biased module.

Some initially tested cells presented clear wormlike visual damage after reverse stress. The worms appeared between the metal grid and the isolating circumference scribe. However, the cells that were part of the controlled study only showed local spot damages, if any, after reverse stress. Cells with a P1 scribe line in the Mo *did not* show a tendency for the damage to appear over the P1 line.

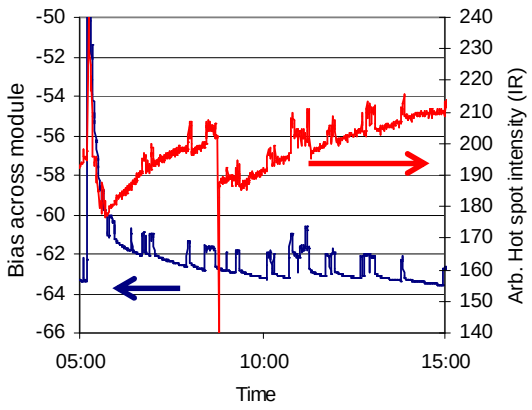

Figure 2 – IR thermography (red) compared with voltage drop (blue) across a module in reverse bias (group B). Momentary ignitions of hot spots (local peaks in intensity) correlate with a drop in voltage across the module.

3.2 Observations of the reverse stress development

The reverse characteristics of modules varied between samples quite significantly. Breakdown voltages between -2V/cell to -4V/cell were found. Single cells showed similar results, with a reverse breakdown between -2V and -4V.

The evolution of reverse bias was monitored and some characteristic differences were noted depending on the testing conditions, i.e. light vs. dark and the level of reverse current. Modules biased in light differed significantly in the bias level, as expected, due to the light current generated in the illuminated samples. At low reverse currents the bias was stable throughout the test, whereas the bias dropped slightly during the first 5 minutes of testing when forcing the full Jsc current through the modules. The magnitude of the drop was in the range of 0.2V/cell. It is likely that this behaviour is due to heating from the light source.

Modules biased in the dark tended to increase their blocking behavior, requiring an increasing level of reverse bias to drive the set current. This effect was modest and in the range of 0.2V increase per cell. For modules set to a reverse current corresponding to ½*Jsc, the bias level exhibited temporary and distinct bias drops in the range of ~1V lasting for a number of seconds (see lower curve in Figure 2). These were related to hot spot activity as shown below in section 3.4.

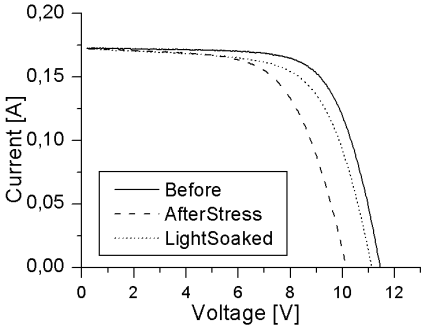

Figure 3 – IV-curve of group C module before (solid) and after (dashed) reverse bias stress. The middle curve (dotted) shows recovery of Voc after forward biased light soaking.

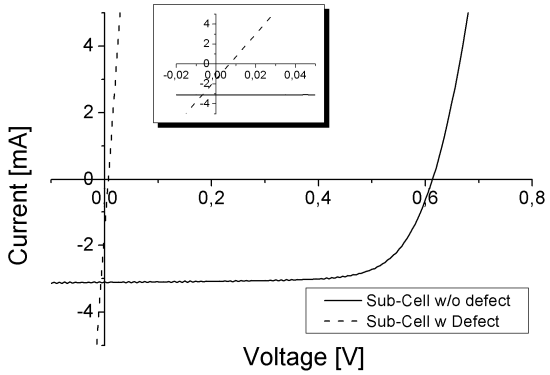

Figure 4 – Comparing small cells sectioned from a reverse biased module. The solid line represents a sub-cell without damage and the dashed line a sub-cell with damage. Inset is an enlarged view at low voltage.

3.3 IV performance

The IV characterization showed the expected losses in FF and Voc for all conditions tested. FF losses were of the magnitude 5-10% of the initial value for all samples, except a few cells whose losses were more pronounced. Although cells with P1 scribe in the back contact did not show any appreciably visible difference to those without, their performance suffered more from the reverse stress. Since no clear trends could be observed for the cell samples, the following discussion is focused on the module results.

The Voc loss was most severe for the module samples biased under light at high current, group **C**, dropping by 10%. However, this Voc loss recovered to almost the level of the other groups under forward biased light soaking for 30 min. For modules stressed in the dark there was no tendency to recover. In spite of the visually apparent difference between groups **A** and **B** (see above), they exhibit similar performance loss.

The main FF loss appears to be due to a decrease in shunt resistivity which does not recover (Figure 3). Indeed, sectioning modules into small (approx. 3x3mm^2) sub-cells with and without the visible damages revealed how the visible damage acts as a strong local shunt. When separated, sub-cells adjacent to the area identified as damaged show good performance, underlining that the effect is localized (Figure 4).

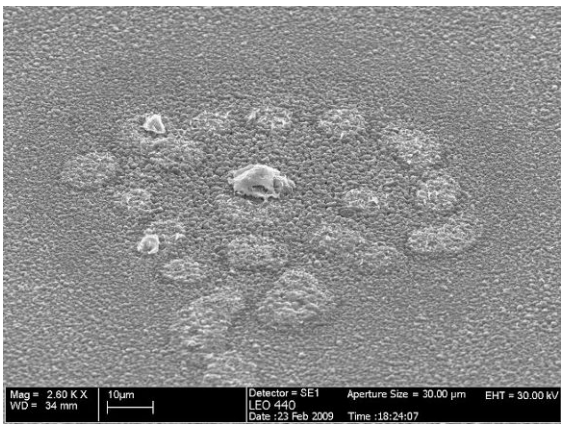

Figure 5 – Point of origin for wormlike damage. Propagation of the damage appears as adjacent spots.

3.4 IR thermography

IR thermography was used to observe the growth of the wormlike damage during reverse stressing. Hot spots appeared across the entire surface of the module, clearly lighting up simultaneously as the module reaches reverse breakdown. Hot spots were observed in each cell. In contradiction to the assumption that the wormlike damage originated in the scribe line [5], we were able to observe how the majority of hot spots originated in the *bulk* of the cell. However, nearly all observed hot spots migrated *towards* the P1 interconnect of the cell where they followed the P1 scribe line and finally stopped at some arbitrary point.

Hot spot activity depended on the level of current being driven through the device. At low levels of current thermography exhibited peaks in intensity, representing hot spots igniting and extinguishing. These were related to changes in the voltage drop across the module. As a hot spot ignited the voltage across the module dropped (see Figure 2). At high levels of current the hot spot activity was more intense and difficult to quantify. Neither thermography nor electrical results showed the distinct features of Figure 2. By matching thermographical traces with photographs of wormlike damages we were able to conclude that they coincided with the appearance and movement of hot spots during reverse stress (see Figure 1a and b).

3.5 SEM/EDX

Closer inspection of the damages showed how they in many cases had a “pearl necklace” appearance consisting of adjacent rings (Figure 5). This would suggest a discreet propagation of the hot spot. Such appearance was not universal; at some places the damaged line showed a more continuous appearance. The points of origin for the damages appeared as heterogeneities in the CIGS material. The nature of such heterogeneities has not been successfully determined and it cannot be conclusively stated that the observed inhomogeneities are the *cause* of the hot spot rather than a *consequence* of a local breakdown and heating of the material. Local heating and material evaporation is supported by the observation that at the points of origin the ZnO layer was often missing as if removed by an explosion.

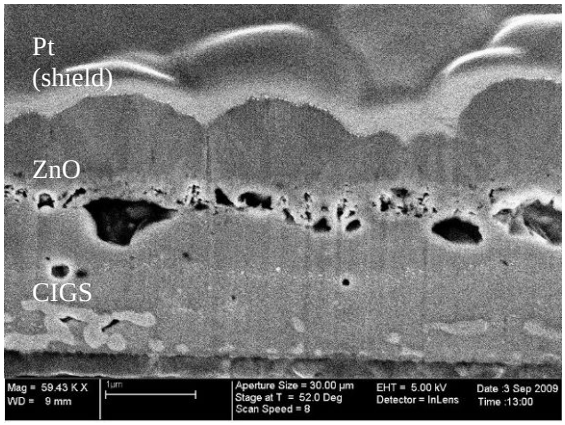

Figure 6 – FIB cross-section of a worm shows how cavities are formed at the absorber/window interface. Note also the segregation of light areas near the back contact.

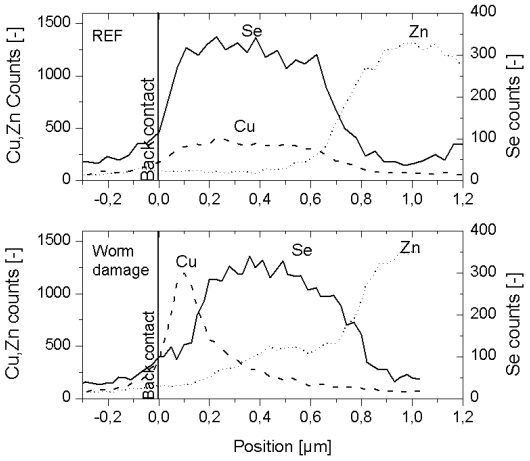

Figure 7 – EDX scan across the layers in the FIB cross section. Mo peak (not present in the graph) set as "0" position. Cross section of the damaged area show how Cu is strong near the back contact and Zn appears to have intermixed with the CIGS layer.

The ZnO window layer was removed by etching in hydrochloric acid. EDX analyses across the damage lines showed that Zn was still present. Cutting through the film using a focused ion beam allowed investigation of change in the layered structure of the solar cell. A section of damaged area is shown in Figure 6. Porosities appear frequently at the top of the CIGS layer. Lighter areas close to the back contact are interpreted as some form of phase segregation in the CIGS. EDX scans across the cross section show a tail of Zn going into the top of the CIGS. Near the back contact, where the lighter areas were observed, the Cu signal increases significantly (see Figure 7).

4 CONCLUSIONS

Visual damages which form during reverse biasing of CIGS modules are related to moving hot spots observed using IR thermography. These hot spots ignite as the module, or cell, reaches a high level of reverse bias and are interpreted as localised breakdowns in the CIGS, possibly due to material inhomogeneities. The path of the hot spots can be seen by visual inspection as wormlike lines in the surface of the device. Hot spot movement is forced when the heating produces evaporation and pore formation at the absorber/window interface. SEM imaging revealed such porosities.

Performance losses due to damage occurred in all module samples. The effect of the damage is an increased local shunt conductance. Samples biased with high current under light show an additional Voc loss which is reversible by forward bias light soaking. Since part of the damage is irreversibly reducing the performance of the device, and also reducing its visual appearance, the need for bypass diodes is strongly supported by these results.

The hypothesis that the P1 scribe causes a weak location for breakdown was not supported by these results, as no preferential hot spot damage was localised to the P1 scribe in the cell experiment.

ACKNOWLEDGEMENTS

The author would like to thank T. Wätjen for FIB work and gratefully acknowledges the support of Solibro Reseach AB as well as the Ångström Solar Center team.

REFERENCES

[1] H. S. Ullal, B. von Roedern, Proc. of 22nd EUPVSEC, (2007), p1926-1929

[2] P. Mack, T. Walter, R. Kniese, D. Hariskos, R. Schäffler, Proc. of 23rd EUPVSEC, (2008), p2156-2159

[3] M. Prorok, S. Ickiewicz, T. Zdanowicz, Proc. of 22nd EUPVSEC, (2007), p2625-2628

[4] C. Köble, J. Klaer, R. Klenk, M.C. Lux-Steiner, Proc. of 21st EUPVSEC, (2006) p1962-1964

[5] E.E. van Dyk, C. Radue, A.R. Gxasheka, Thin Solid Films 515 (2007) p6196– 6199